Desalination and Water Treatment
www.deswater.com
doi: 10.1080/19443994.2014.927187

53 (2015) 887–897
January

Taylor & Francis
Taylor & Francis Group

An experimental study of solar thermal vacuum membrane distillation desalination

Yongqing Wang[a,*], Zhilong Xu[a], Noam Lior[b], Hui Zeng[a]

[a]*Cleaning Combustion and Energy Utilization Research Center of Fujian Province, Fujian Province Key Laboratory of Energy Cleaning Utilization and Development, Jimei University, Xiamen 361021, China, Tel. +86 592 6180597; Fax: +86 592 6183503; email: yongqing@jmu.edu.cn*
[b]*Department of Mechanical Engineering and Applied Mechanics, University of Pennsylvania, Philadelphia, PA 19104-6315, USA, email: lior@seas.upenn.edu*

Received 20 August 2013; Accepted 14 January 2014

ABSTRACT

An experimental desalination system coupling a vacuum membrane distillation (VMD) unit and a vacuum tube solar heat collection (SHC) unit was developed and tested. The parametric sensitivity of the VMD unit performance was investigated first using an electric heater as the heat source, and then the whole system was examined using solar heat. It was revealed that hot feed temperatures higher than 65 °C and cold-side absolute pressure lower than 0.02 MPa are favorable for high trans-membrane flux. The startup time of the SHC-VMD system was very short, less than 10 min. The VMD unit ran intermittently for 305 h in five months, individually or together with the solar heat system, showing good suitability to unsteady solar energy and to the intermittent off-and-on operation mode. The average trans-membrane flux in the experiments of SHC-VMD combined system was about 4 kg/(m^2 h), and the specific heat consumption was around 750 kWh/m^3.

Keywords: Solar thermal desalination; Vacuum membrane distillation; Seawater desalination

1. Introduction

Desalination has been considered to be an important and effective way to mitigate water-shortages in many arid areas in the world. According to the 24th IDA (International Desalination Association) Worldwide Desalting Plant Inventory, the total capacity of completed desalination plants was 71.9 million m^3/d by the end of 2011 [1]. Desalination is an energy-intensive industry that not only depletes the fossil fuels that are typically used as the energy source, but also causes emissions of greenhouse and other undesirable gases. Driving the process by renewable energies is thus an important development goal, as long as the produced water cost is acceptably low. Thermally driven desalination processes can thus be driven by solar or geothermal heat sources.

*Corresponding author.

This paper originated at ECOS 2013 – the 26th International Conference on Efficiency, Cost, Optimization, Simulation and Environmental Impact of Energy Systems held during 15–19 July 2013 in Guilin, China, and was accepted for publication in Desalination and Water Treatment after regular review and required revisions, under the guest editorship of Dr Yingru Zhao from Xiamen University, China

Membrane distillation (MD) desalination is a separation technology combining thermal distillation with membrane separation, where hot feed solution flows at one side of a hydrophobic microporous membrane, with the other side exposed to an environment at a temperature and pressure governed by a cold condenser. The water evaporates due to this potential difference and the vapor penetrates through the membrane pores and is condensed as product water at the cold side. There are mainly four types of MD processes, with the principles shown in Fig. 1. Hot feed solution is in direct contact with one side of the membrane in all MD configurations and the differences among them lie in the nature of the cold side of the membrane: in direct contact membrane distillation (DCMD), a cold distilled water stream is used to collect the water vapor penetrating from the hot side of the membrane; in vacuum membrane distillation (VMD) and sweeping gas membrane distillation (SGMD), the vapor is swept away by vacuuming and by gas stripping, respectively, and then condensed usually in a separate condenser; and in air gap membrane distillation (AGMD), an air gap is interposed between the membrane surface and the condensing surface. All the configurations of MD can be applied to seawater or brackish water desalination, while the most commonly used are DCMD, AGMD, and VMD [2].

Compared with other desalination processes, the main features of MD include high system compactness, high product water quality same as that characteristic to distillation processes, low sensitivity to feed concentration, and the ability to run at low temperatures [3,4]. The typical operating temperature of MD is in the range of 60–80°C [5], a temperature level dictated by the upper temperature limits of the membranes typically used in MD and at which, coincidentally, solar thermal collectors work economically and well. Many of the existing MD experimental and pilot units are indeed driven by solar heat [5–14].

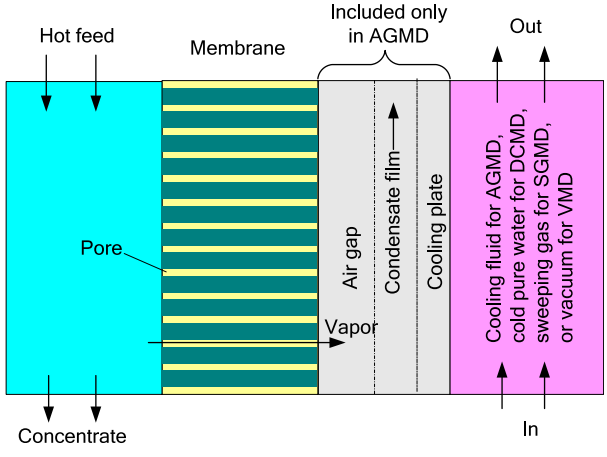

Fig. 1. Principle of four types of MD configurations.

The published studies on solar heat-powered MD system were on small-scale units, of capacity below 2,000 L/d. Two different layouts were developed: compact system, where the MD feed solution is heated directly in the solar thermal collector, and two-loop system, where the feed solution is heated indirectly in a heat exchanger by the hot fluid from the solar thermal collector. Table 1 summarizes the general information of the pilot plants and experimental set-ups built in the past decade. Most of the systems had very low recovery ratio (mass ratio of the produced water and the feed solution), lower than 7%, and high thermal energy consumption of water production, higher than 200 kWh/m^3. By recycling the concentrated brine as feed, the system reported in [12] had a recovery ratio up to 55%, comparable to traditional multi-stage flash and multi-effect distillation (MED) systems. Owing to the effective condensation heat recovery inside the MD module and sensible heat recovery by brine recycling, the system [12] also had the lowest heat consumption, 140–350 kWh/m^3, among the systems listed, which is still much higher than that of the mature thermal desalination technologies, such as MED with heat energy consumption of 40–65 kWh/m^3 [11]. A comprehensive review and evaluation of solar MD systems is available in [15,16].

The objective of the present work was to investigate experimentally the performance of a solar desalination system coupling a vacuum tube solar collector and a VMD unit. The experimental set-up was built in Xiamen, a seaside city in the southeast of China, with an average daily insolation of 12.6 MJ/m^2/d [17]. The VMD unit used was first tested and examined using an electric heater, and then using the solar collector heater, as a combined system.

2. The experimental set-up

Fig. 2 shows the schematic diagram of the experimental system, where the two subsystems, the solar heat collection (SHC) unit and the VMD unit, are interconnected by a titanium plate heat exchanger where feed seawater for the VMD is heated by the hot water from the SHC. Fig. 3 gives the photographs of the solar collector and the VMD unit.

The SHC subsystem mainly consists of a vacuum tube collector with aperture area of 2.16 m^2 (Fig. 3), a hot water tank with capacity of 500 L, and a

Table 1
General information of some established solar-powered MD systems

Reference number	[6]	[7]	[8]	[9]	[10]	[5]	[11]	[5,12]	[13]
Geographic location	Freiburg, Germany	Aqaba, Jordan	Irbid, Jordan	Alexandria, Egypt	Hangzhou, China	Gran Canaria, Spain	Almería, Spain	Gran Canaria, Spain	Almería, Spain
System layout	Compact	Two-loop	Compact	Compact	Compact	Two-loop	Two-loop	Compact	Two-loop
MD configuration	AGMD	AGMD	AGMD	AGMD	VMD	AGMD	AGMD	PGMD[d]	AGMD
Membrane material	PTFE	PTFE	PTFE	PTFE	PP	PTFE	PTFE	PTFE	N/A
Membrane area, m^2	8	40	10	N/A	0.09	35–60[c]	2.8	8.5–10[e]	9
Solar collector type	N/A[a]	Flat plate	Flat plate	Flat plate	N/A	Flat plate	CPC	Flat plate	CPC
Collector area, m^2	5.9	72	5.73	5.73	8	90	500	6.96	500
Electricity source	Grid	PV	PV	PV	Grid	PV	Grid	PV	Grid
Type of feed water	Tap water	Seawater	N/A	Brackish	Brackish	N/A	NaCl solution	Seawater	NaCl solution
Hot feed temp., ℃	~ 90	N/A	N/A	N/A	55.5–83	N/A	~ 90	~ 86	~80; ~85[f]
Distillate conductivity, μS/cm	N/A	20–250	5	3	~4	N/A	12–60	20–200	2–5
Water output, L/d	~130	144–792[b]	~ 120	64	~15.6[b]	1,200	N/A	5–120	N/A
Water flux per m^2 membrane, kg/m^2 h	~1.88[b]	~1.5	~2.5	N/A	~32.19	N/A	~6.5	N/A	~5.09
Salt retention rate, %	N/A	>98	N/A	99.5	>98.3[b]	N/A	99.9[b]	88–99.9	>99.8
Recovery ratio, %	~6.7[b]	2–4.5	1–4	N/A	0.25–1.6[b]	N/A	N/A	0.1–55	0.3–1.8; 2.2–4.5[f]
Heat consumption, kWh/m^3	N/A	200–300 (926–1,389)[g]	200–300 (718–2,153)[h]	N/A	7,850 [15]	N/A	810–2,200	140–350	1805~; 294~[f]
Running period	Few months	Few months	Few months	6 months	Within one month	N/A	4 months	907 days in five years	7 months; 3 months[f]

[a]N/A = Not available.
[b]Values calculated from the reported data.
[c]The MD unit had five modules, and each module had a membrane area of 7–12 m^2.
[d]PGMD is the abbreviation of permeate gap membrane distillation, an enhanced configuration of DCMD [12].
[e]The membrane area was 8.5 m^2 at first, and then changed to 10 m^2.
[f]The first data is for prototype A in which the MD was a single-stage design, and the second data is for prototype B in which three stages of MD modules were connected in series.
[g]Value calculated from the performance ratio, 0.2–0.3 kg/MJ, reported in the paper, which is contradictory against claimed 200–300 kWh/m^3.
[h]Value calculated from the gained output ratio, 0.3–0.9, reported in the paper, which is contradictory against claimed 200–300 kWh/m^3.

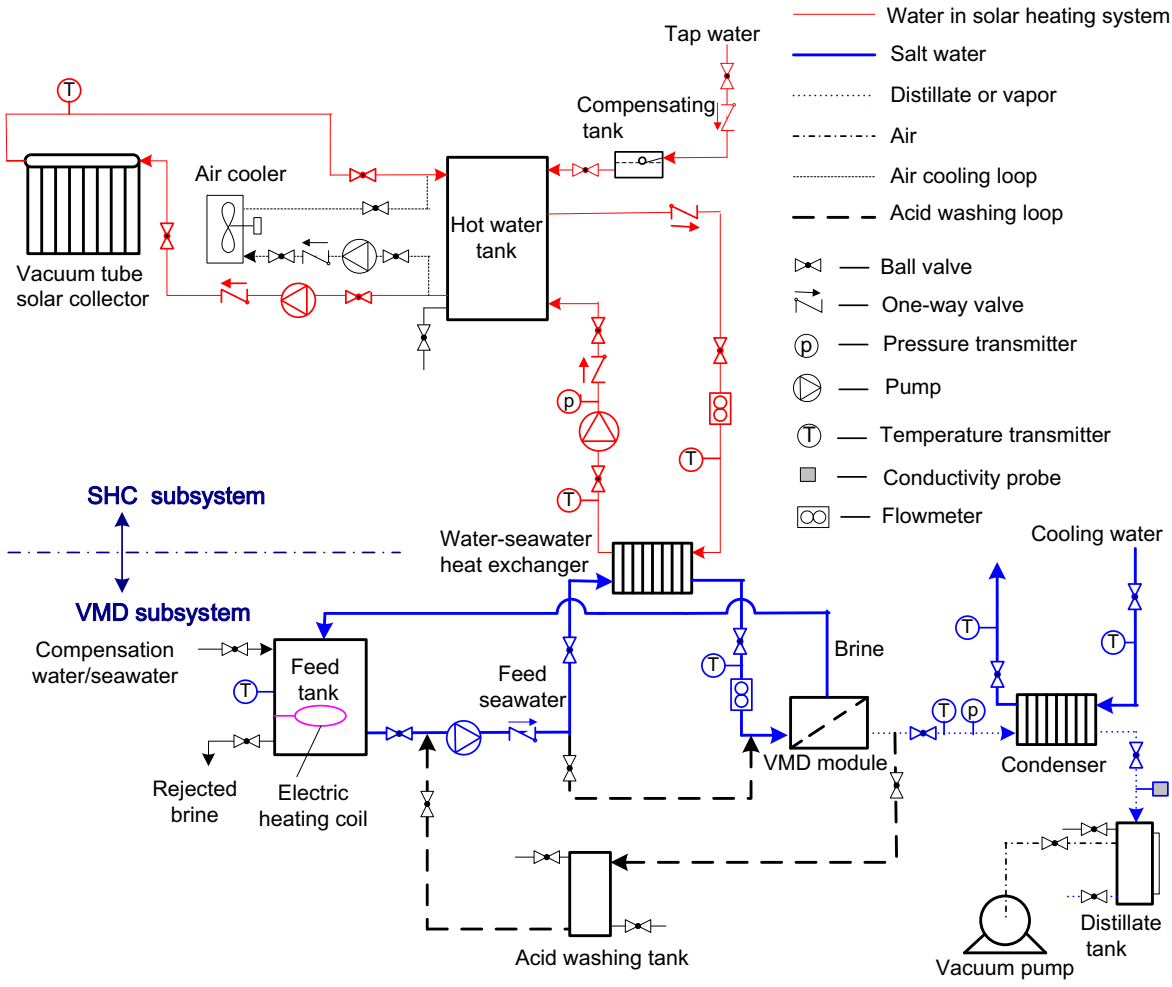

Fig. 2. Schematic diagram of the SHC-VMD system.

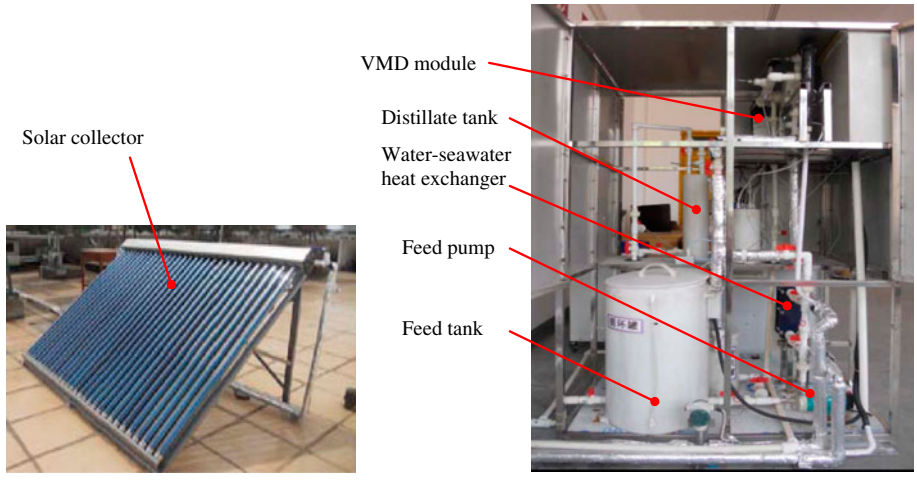

Fig. 3. Photographs of the solar thermal collector and the VMD unit.

compensating tank for water replenishment. The solar collector was manufactured by Shengyuan New Energy Corp., China [18]. Thirty glass vacuum tubes with an outer diameter of 47 mm and effective length of 1,640 mm were used. Tap water is the working fluid used in the SHC, heated in the solar collector, and then returns to the hot water tank. The heated water is pumped through the water–seawater heat exchanger, releasing heat to the feed seawater, and then returning to the water tank. An air cooling loop, shown as dotted line in Fig. 2, is also included in SHC, to protect the solar collector from overheating in hot weathers when the experimental set-up is idle.

In the VMD subsystem, hot seawater from the water–seawater heat exchanger enters the VMD module which was manufactured by the Tianjin Hydroking Science and Technology Ltd, China [19]. The module is rectangular, with internal dimensions of 75 mm long, 75 mm wide, and 50 mm high. The construction of the module can be found in [20]. The membrane used is hollow fiber polypropylene with nominal pore size of 0.2 μm, porosity of 50–60%, and thickness of 220 μm. The effective membrane area for vapor transport is 0.25 m^2. Hot seawater cross-flows over the outside surface of the membrane fibers as illustrated in [20]. Driven by the vapor pressure difference between the liquid/vapor interface at the hot side of the membrane and the vacuum maintained by the vacuum pump at the other side, water vapor passes through the membrane, thus separating the feed seawater into water vapor and concentrated brine. The water vapor is condensed in the condenser and then collected in the distillate tank. The brine flows back to the feed tank where seawater or distilled water at ambient temperature is added to keep a constant water level.

Running the system with seawater compensation, the feed concentration will increase until it reaches a certain value, say 70–100 g/kg, and then the drain valve at the bottom of the feed tank is opened to reject part of the concentrated brine. The feed concentration is kept constant by adding appropriate amounts of distilled water, making it convenient to study the performance of VMD at a desired salt concentration of feed. An acid-washing loop for membrane cleaning, shown as dotted line at the bottom of Fig. 2, is included in the VMD subsystem. It runs only when the conductivity of the produced distillate is above a certain value, say higher than 100 μS/cm, and uses a dilute aqueous solution of HCl with concentration lower than 0.05 mol/L as cleanser. An electric heating coil made of titanium is installed in the feed tank, making it possible to provide heat for the process to also examine the performance of VMD independently from solar heating.

The experimental set-up was monitored online with the instruments for temperature, pressure, flow rate, and conductivity measurement at locations shown in Fig. 2. The instruments used and their uncertainties are shown in Table 2. The differential pressure transmitter BL-C3051 was used to measure the water level of the distillate tank, from which the water mass in the tank was calculated by the computer connected.

3. Experimental results and discussions

3.1. Performance of the VMD unit

To understand the water production and parameter selection of the VMD unit used here, the performance of VMD was examined first, using electricity instead of solar energy as driving heat source. An aqueous NaCl solution with salt concentration from 35 to 45 g/kg was used to simulate seawater. An on-off temperature controller was used to control the feed temperature of the feed tank.

Table 2
Measuring instruments used in the experiments

Instrument	Type	Manufacturer	Range	Uncertainty (% of full scale)
Pressure transmitter	BL-Y202	BILY, China	−0.1–0 MPa	±0.5
Thermal resistance transmitter	Pt100	BILY, China	0–200 °C	±0.25
Differential pressure transmitter	BL-C3051	BILY, China	0–4.9 kPa	±0.5
Conductivity probe	CM-230	CREATE, China	0–199.9 μS/cm	±1.5
Paddlewheel flow meter	F3.00	FLS, Italy	Flow velocity: 0.15–8 m/s	±0.75
Solar power meter	TM207	TENMARS, Taiwan	0–1999 W/m^2	±0.5

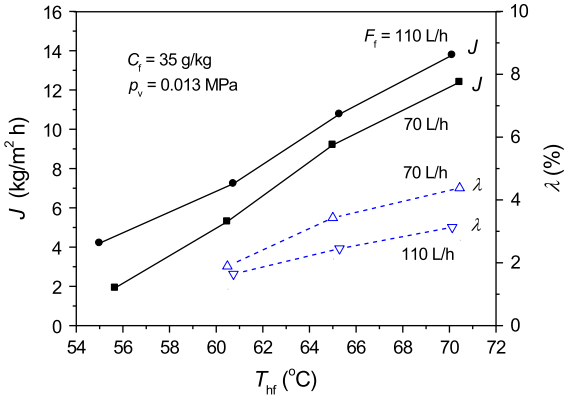

Fig. 4. Effect of hot feed temperature T_{hf} on trans-membrane flux J and recovery ratio λ of VMD (using electricity as heat source), for different feed flow rates F_f.

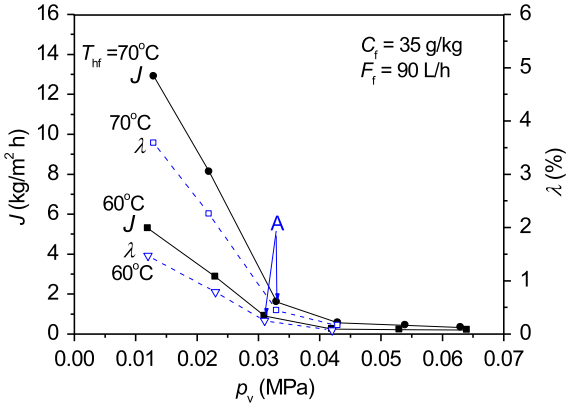

Fig. 5. Effect of cold-side absolute pressure p_v on trans-membrane flux J and recovery ratio λ of VMD (using electricity as heat source), for different feed temperatures T_{hf}.

The effects of the fundamental operation parameters, including the temperature of hot feed solution at MD module inlet T_{hf}, the cold-side absolute pressure p_v, the feed flow rate F_f, and the feed concentration C_f, on the trans-membrane flux J which is the main performance index of MD unit and defined as the permeate mass penetrating per m^2 membrane area per unit time, and on the recovery ratio λ which is the mass ratio of the produced water and the feed solution, were studied experimentally with the results illustrated in Figs. 4–7. During the experiments, distilled water was continuously added to the feed tank at rates needed to keep the C_f constant. It is clear that although the concentrated brine was recycled to the feed tank, the working condition of the VMD module was the same as that in a once-through desalination system, other than a recirculation system where the feed concentration is always increasing. That is why the recovery ratios of once-through system are shown in Figs. 4–7. Within the parameter range of T_{hf} = 55–75 °C, p_v = 0.01–0.02 MPa, F_f = 70–110 L/h, and C_f = 30–45 g/kg, the relative uncertainty in both J and λ was estimated to be less than 5%, as shown in Appendix A.

It was found that T_{hf} and p_v are the main factors influencing J. Increasing T_{hf} results in greatly increased J (Fig. 4): for example, increasing T_{hf} from 55 to 70 °C would increase J from 1.9 to 12 kg/(m^2 h) for p_v = 0.013 MPa, F_f = 70 L/h, and C_f = 35 g/kg. The reason is that higher T_{hf} leads to exponentially increased water vapor pressure at the hot side of the membrane, thus causing larger mass transfer driving force for vapor penetration. Increasing T_{hf} by 1 °C could increase J by 0.14–0.86 kg/(m^2 h) in this work.

Table 3
Pressure at turning point A and characteristics of feed solution for different cases

Case number	1	2	3	4	5	6	7
Reference number	[24]			[25]		This work	
Type of feed solution	Waste water from oil field			NaCl solution		NaCl solution	
Salt concentration of feed	21.5 g/L			3.58 g/kg		35 g/kg	
Temperature of hot feed T_{hf}, °C	40	50	60	45	55	60	70
Boiling point elevation of feed ΔT_b, °C	0.21[a]	0.22[a]	0.24[a]	0.036[a]	0.038[a]	0.41	0.43
Saturation pressure of feed p_{sf}, MPa	0.0071[a]	0.0122[a]	0.0197[a]	0.0096[a]	0.0157[a]	0.0196	0.0306
Cold-side vacuum pressure at point A, MPa	0.087[b]	0.08[b]	0.07[b]	0.076[b]	0.073[b]	0.07	0.068
Cold-side absolute pressure at point A p_{vA}, MPa[c]	0.014	0.021	0.031	0.025	0.028	0.031	0.033

[a]Values calculated using reported data.
[b]Values read from reported figures.
[c]Values calculated taking ambient pressure as 0.101 MPa.

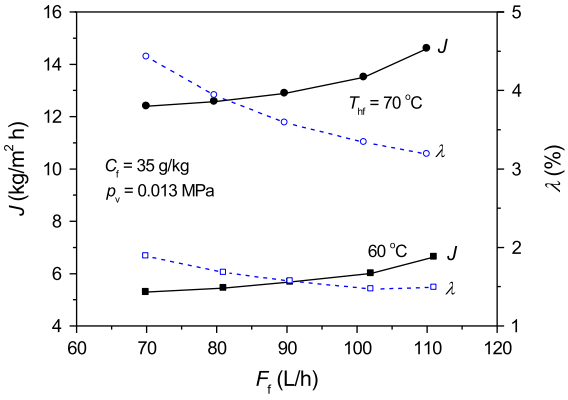

Fig. 6. Effect of feed flow rate F_f on trans-membrane flux J and recovery ratio λ of VMD (using electricity as heat source), for different feed temperatures T_{hf}.

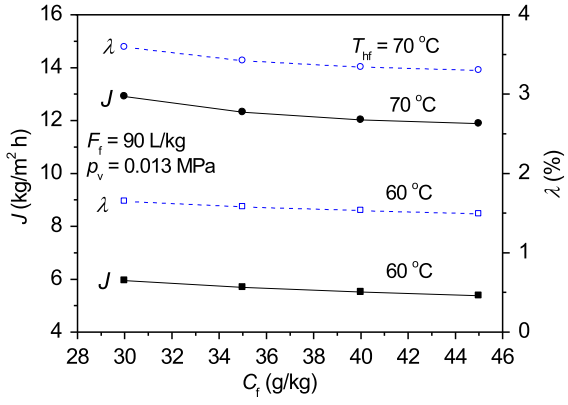

Fig. 7. Effect of feed concentration C_f on trans-membrane flux J and recovery ratio λ of VMD (using electricity as heat source), for different feed temperatures T_{hf}.

Decreasing the cold-side absolute pressure p_v also leads to higher J (Fig. 5), because the driving force of mass transfer increases with the decrease of p_v. Different from the results reported in many publications (cf. [21,22]) where J showed nearly linear relation with p_v, our results show that J rises very slightly at higher p_v, but when p_v is lower than a certain value, J tends to rise sharply. The trend is similar to that in [23–25]. Based on the available experimental data in [24,25] and this work, Table 3 summarizes the cold-side pressure p_{vA} at point A (as indicated in Fig. 5) and the saturation pressure p_{sf} of the hot side feed solution. Kuang et al. [25] attributed the sharp increase of J under $p_v \le p_{vA}$ to the vaporization behavior change of the hot side solution from surface evaporation to intense boiling, but to the authors' knowledge, no one has studied the possibility of boiling in VMD or observed the phenomena in experiments so far. Obviously, only when $p_v \le p_{sf}$, boiling may occur, but in all the cases shown in Table 3, $p_{vA} > p_{sf}$ (for example, $p_{vA} = 0.014$ MPa and $p_{sf} = 0.007$ MPa in Case 1, and $p_{vA} = 0.021$ MPa and $p_{sf} = 0.012$ MPa in Case 2), which means that high increase rate of J can also be obtained when the hot side fluid is at certain subcooled states (when 0.007 MPa $< p_v <$ 0.014 MPa in Case 1 and 0.012 MPa $< p_v <$ 0.021 MPa in Case 2, for instance). Further study is needed to clarify the reason. It is clear that lower p_v should be chosen to pursuit higher water production, and as to the VMD unit used here, p_v lower than 0.02 MPa is more suitable.

The influence of the feed flow rate F_f is not as significant as T_{hf} and p_v (Fig. 6). For instance, increasing F_f from 70 to 110 L/h (with increase rate of 57%), J only increases from 12.4 to 14.4 kg/(m^2 h) (with increase rate of 16%), under $T_{hf} = 70$°C, $p_v = 0.013$ MPa, and $C_f = 35$ g/kg. An increase in F_f implies a higher velocity of the feed solution, thus enhancing the heat and mass transfer in the boundary layer on the membrane surface and reducing the effect of the temperature and concentration polarization, and hence results in an increased rate of J.

Keeping the other conditions constant, Fig. 7 shows the experimental results for different feed salt concentration C_f changing from 30 to 45 g/kg, which is the typical salinity range of seawater in the world. J decreases with the increase of C_f. The main reason is that higher C_f leads to lower water activity (defined as vapor pressure ratio of salt solution and pure water with the same temperature) and higher concentration polarization, resulting in lower water vapor pressure at the hot side of the membrane and then lower vapor pressure difference between the two sides of the membrane. It is also shown that the membrane used here has low sensitivity to the salt concentration. For instance, increasing C_f from 30 to 45 g/kg (with increase rate of 50%), J only decreases from 12.9 to 11.9 kg/(m^2 h) (with decrease rate of 7.7%) under $T_{hf} = 70$°C, $p_v = 0.013$ MPa, and $F_f = 90$ L/h.

As shown in Figs. 4–7, the recovery ratio λ of the VMD unit is very low, lower than 5% within the parameter range studied, which is comparable to the results in other publications [7,8,10,13], as shown in Table 1. This means that in the once-through MD unit, only less than 5% of the feed mass is output as product water, and the balance, which accounts for more than 95% of the feed mass and has a salinity less than 5% higher than that of the feed, is rejected. Because of the low sensitivity of MD to the salinity of feed solution, recycling part of the concentrate can be an effective way to increase λ and then reduce the feed pretreatment cost. For example, λ would nearly double when the recirculating flow is set at 50% of the feed

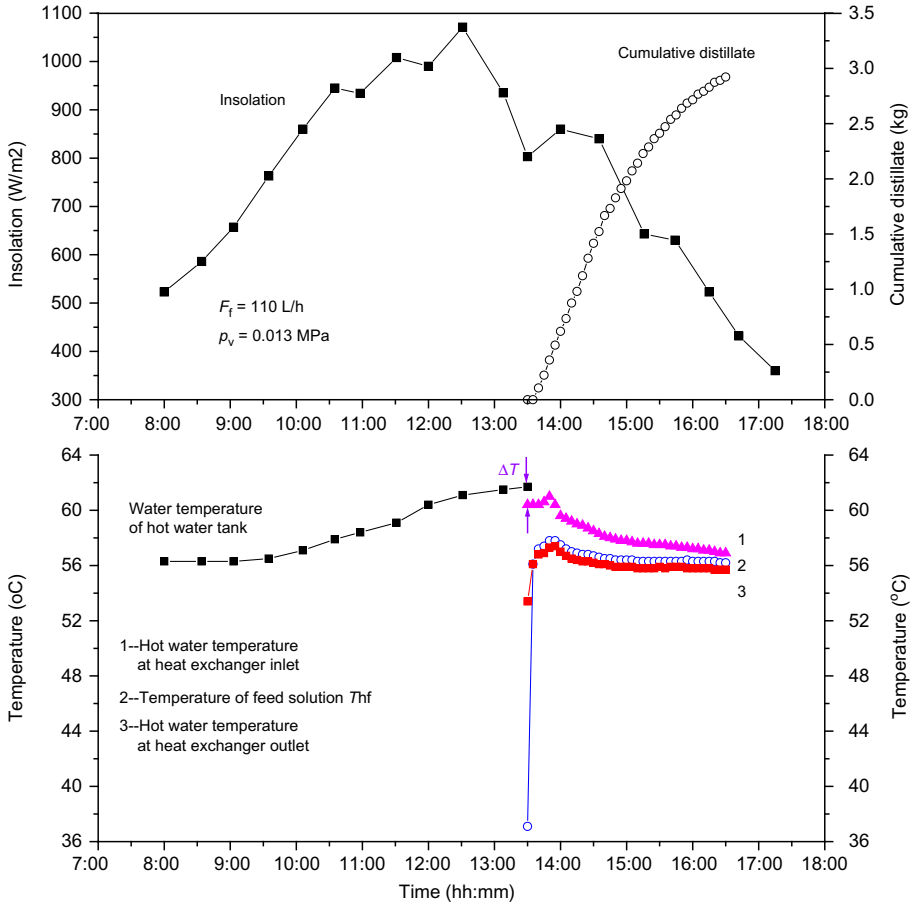

Fig. 8. Experimental results of SHC-VMD on Aug. 14, 2012.

flow. In the system reported in [12], only a small amount of brine left the system, and the balance returned to the system as feed, resulting in a high recovery ratio up to 55%.

The salt concentration of the produced water was found by measuring its electrical conductivity online within the experimental parameter range of T_{hf} = 55–75 ℃, p_v = 0.01–0.03 MPa, F_f = 70–110 L/h, and C_f = 30–45 g/kg, respectively, and the values obtained were lower than 30 μS/cm, which corresponds to a salt concentration of about 0.018 g/kg (18 ppm by wt.) [26], indicating that the salt retention rate of the VMD unit is higher than 99.9%. This is comparable to the results reported by others as those shown in Table 1.

3.2. Performance of the SHC-VMD system

The experiments of the SHC-VMD system were carried out in August 2012. As an example, Fig. 8 gives the results obtained on August 14, during which the system ran for 3 h, from 13:30 to 16:30. The NaCl solution with a concentration of 35 g/kg was used, and by compensating the same solution (other than distilled water as in the experiments in Section 3.1), the feed concentration increased continuously and reached 36.5 g/kg at the end of the experiment. About 3 kg of fresh water was produced. The average transmembrane flux was 4 kg/(m^2 h), higher than that reported in [6–8], but lower than that in [11] and [13] (Table 1). The average water production corresponding to per m^2 collector area was 0.46 kg/h.

In Fig. 8 it can be seen that the temperature of the water in the hot water tank remained almost constant before 9:30, which was because the collector was shaded until then by an adjacent wall. The temperature began to increase after that when the collector became exposed to the insolation, and reached about 62 ℃ at 13:30. The temperature drop, indicated by ΔT in Fig. 8, between the water in tank and the heat exchanger inlet was due to insufficient insulation around the connecting pipe. The hot water from the hot water tank provided the heat energy for VMD by

lowering its temperature in the water–seawater heat exchanger. Using numerical integration, the amount of the heat energy was determined by calculating the heat energy supplied in each minute based on the temperature variation and the flow rate of the hot water, and then adding up all the results. Dividing the sum by the produced water mass, the specific thermal energy consumption was found to be around 2,700 kJ/kg, that is, 750 kWh/m^3.

There are generally two ways to lower the heat consumption of water production in MD systems: recovering the sensible heat of concentrated brine by brine recirculation, and recovering the condensation heat using feed solution in the condenser. Running as a simple cycle, the heat consumption of the system reported in [10] was as high as 7,850 kWh/m^3. Applying the brine recirculation, our system and that in [11] obtained much lower value, 750 and 810–2,200 kWh/m^3, respectively. Using both ways of energy recovery further lowered energy consumption, to 140–350 kWh/m^3 [12]. The design of the energy recovery module is also very important. For example, both sensible and latent heat recovery were applied in the two prototypes in [13], but Prototype B had much lower energy consumption (>294 kWh/m^3) than Prototype A (>1,805 kWh/m^3), mainly because a more efficient three-stage configuration was used.

Solar energy is inherently unsteady, and it is desired that the systems driven by it should work well under variable working conditions and intermittent operation modes. The experiments performed here prove again the suitability of combining MD and solar energy. Firstly, in the experiments performed, the VMD unit was always able to adjust itself to parameter changes in heat source, cooling water, and the ambient. Secondly, the start-up time of the experimental system is very short, less than 10 min. In the case shown in Fig. 8, it took only five minutes to raise the temperature of the feed solution from 37 to 56℃ after starting the hot water pump, and two minutes later the produced water appeared in the distillate collection tank. Thirdly, the VMD unit ran, individually or together with the SHC, for 305 h in five months intermittently, with the performance remaining basically the same as that at the initial time. Dry up of membrane during shutdown periods and the intermittent off-and-on operation seem to have little influence on the membrane and the VMD unit.

The experiments also show that even in good weather conditions, the available solar radiation does not allow this SHC-VMD system to produce water for more than four hours a day, and that the average trans-membrane flux is only around 4 kg/(m^2 h) (membrane area based), which is much lower than the 14.4 kg/(m^2 h) (Fig. 6) that the VMD unit can reach with steady heat supply. The reason for the low permeate flux is the low temperature of the feed solution, which was only 55.9–57.8℃ in the case shown in Fig. 8, while that for a suitably high permeate flux should be above 65℃ (Fig. 4). One of the main reasons for the undesirably low temperature of hot water is the inadequate area of the chosen solar collector. For example, assuming that the mean insolation is 700 W/m^2, the insolation time is 8 h a day, and 60% of the insolation is converted into the energy of water in the water tank, the collector used can increase the water temperature by only 12.5℃. More studies and experiments with larger collectors are in planning to make clear (1) whether the vacuum tube collector used is capable of providing hot water with temperatures above 65℃ under the climatic conditions of Xiamen, and (2) the relation among the collector area, the capacity of MD unit, and the water cost.

4. Conclusions

Based on the SHC-VMD experimental set-up developed, experiments were carried out on the VMD unit and the whole system, with the results reported and discussed in this paper.

An aqueous NaCl solution with concentration of 30 to 45 g/kg was used as feed. The VMD module showed a trans-membrane flux up to 14.4 kg/(m^2 h). The hot feed temperature and the cold-side absolute pressure of the membrane are the main factors influencing the trans-membrane flux, and feed temperature over 65℃ and cold-side absolute pressure lower than 0.02 MPa are favorable for high water flux, higher than 7 kg/(m^2 h). More than 99.9% of salt in the feed was rejected by the membrane. The recovery ratio of the once-through VMD unit was very low, lower than 5%. The low sensitivity of VMD to the feed concentration provides an effective way to improve the recovery ratio by brine recycling.

The startup time of the SHC-VMD system was very short, less than 10 min. The VMD unit ran for 305 h in five months, individually or together with the SHC subsystem, showing good suitability to unsteady solar energy and to the intermittent off-and-on operation mode. The average trans-membrane flux was around 4 kg/(m^2 h) and the specific heat consumption around 750 kWh/m^3 in the experiments of SHC-VMD combined system.

Acknowledgments

The authors gratefully acknowledge the support of the Natural Science Foundation of Fujian Province, China (Project No. 2012J01227), the Educational Department of Fujian Province, China (Project No. JA10193), and the Foundation for Innovative Research Team of Jimei University, China (Project No. 2009A002).

Nomenclature

C_f — salt concentration of feed solution, g/kg
F_f — flow rate of feed solution, L/h
J — trans-membrane flux based on per m^2 membrane area, $kg/m^2 h$
p_{sf} — saturation pressure of hot feed solution, MPa
p_v — absolute pressure at the cold-side of membrane, MPa
T_{hf} — temperature of hot feed solution at MD module inlet, ℃
λ — recovery ratio of MD unit, %
ΔT_b — boiling point elevation, ℃

References

[1] http://www.desalyearbook.com/market-profile/11-global-capacity [accessed on 29 December 2013].
[2] E.K. Summers, H.A. Arafat, J.H. Lienhard, Energy efficiency comparison of single-stage membrane distillation (MD) desalination cycles in different configurations, Desalination 290 (2012) 54–66.
[3] A.M. Alklaibi, N. Lior, Membrane-distillation desalination: Status and potential, Desalination 171 (2004) 111–131.
[4] Y. Kim, K. Thu, N. Ghaffour, K.C. Ng, Performance investigation of a solar-assisted direct contact membrane distillation system, J. Membr. Sci. 427 (2013) 345–364.
[5] J. Koschikowski, M. Wieghaus, M. Rommel, V.S. Ortin, B.P. Suarez, J.R.B. Rodríguez, Experimental investigations on solar driven stand-alone membrane distillation systems for remote areas, Desalination 248 (2009) 125–131.
[6] J. Koschikowski, M. Wieghaus, M. Rommel, Solar thermal-driven desalination plants based on membrane distillation, Desalination 156 (2003) 295–304.
[7] F. Banat, N. Jwaied, M. Rommel, J. Koschikowski, M. Wieghaus, Performance evaluation of the "large SMADES" autonomous desalination solar-driven membrane distillation plant in Aqaba, Jordan, Desalination 217 (2007) 17–28.
[8] F. Banat, N. Jwaied, M. Rommel, J. Koschikowski, M. Wieghaus, Desalination by a "compact SMADES" autonomous solarpowered membrane distillation unit, Desalination 217 (2007) 29–37.
[9] H.E.S. Fath, S.M. Elsherbiny, A.A. Hassan, M. Rommel, M. Wieghaus, J. Koschikowski, M. Vatansever, PV and thermally driven small-scale, stand-alone desalination systems with very low maintenance needs, Desalination 225 (2008) 58–69.
[10] X. Wang, L. Zhang, H. Yang, H. Chen, Feasibility research of potable water production via solar-heated hollow fiber membrane distillation system, Desalination 247 (2009) 403–411.
[11] E. Guillén-Burrieza, J. Blanco, G. Zaragoza, D. Alarcón, P. Palenzuela, M. Ibarra, W. Gernjak, Experimental analysis of an air gap membrane distillation solar desalination pilot system, J. Membr. Sci. 379 (2011) 386–396.
[12] R.G. Raluy, R. Schwantes, V.J. Subiela, B. Peñate, G. Melián, J.R. Betancort, Operational experience of a solar membrane distillation demonstration plant in Pozo Izquierdo-Gran Canaria Island (Spain), Desalination 290 (2012) 1–13.
[13] E. Guillén-Burrieza, G. Zaragoza, S. Miralles-Cuevas, J. Blanco, Experimental evaluation of two pilot-scale membrane distillation modules used for solar desalination, J. Membr. Sci. 409–410 (2012) 264–275.
[14] J.R.B. Rodríguez, V.M. Gabet, G.M. Monroy, A.B. Puerta, I.F. Barrio, Distilled and drinkable water quality produced by solar membrane distillation technology, Desalin. Water Treat. 51 (2013) 1265–1271.
[15] R.B. Saffarini, E.K. Summers, H.A. Arafat, J.H. Lienhard V, Technical evaluation of stand-alone solar powered membrane distillation systems, Desalination 286 (2012) 332–341.
[16] M.R. Qtaishat, F. Banat, Desalination by solar powered membrane distillation systems, Desalination 308 (2013) 186–197.
[17] Climatic Data Center of China Meteorological Administration and Department of Building Science and technology in Tsinghua University, Meteorological data set for thermal environment analysis of buildings in China. China Architecture & Building Press, Beijing, 2005 (in Chinese).
[18] Vacuum Tube Solar Collector. Shengyuan New Energy Corp., China. http://sytyn.com/ [accessed 29 December 2013].
[19] Vacuum Membrane Distillation Module. Tianjin Hydroking Science and Technology Ltd, China. http://www.hydroking.com.cn/ [accessed 29 December 2013].
[20] B. Li, K.K. Sirkar, Novel membrane and device for vacuum membrane distillation-based desalination process, J. Membr. Sci. 257 (2005) 60–75.
[21] M. Safavi, T. Mohammadi, High-salinity water desalination using VMD, Chem. Eng. J. 149 (2009) 191–195.
[22] J.P. Mericq, S. Laborie, C. Cabassud, Vacuum membrane distillation for an integrated seawater desalination process, Desalin. Water Treat. 9 (2009) 287–296.
[23] X. Wang, Preparation of PVDF hydrophobic membrane and study on membrane distillation integrated technique [dissertation], Zhejiang University, China, 2008 (in Chinese).
[24] C. Wang, J. Zhong, J. Wang, Desalination of oil-field waste water via vacuum membrane distillation, Membr. Sci. Technol. 24(1) (2004) 46–49 (in Chinese).
[25] Q. Kuang, L. Li, L. Min, Y. Ding, Desalination of Luobupo bitter and salty water by vacuum membrane distillation, Membr. Sci. Technol. 27(4) (2007) 46–49 (In Chinese).

[26] F. Banat, R. Jumah, M. Garaibeh, Exploitation of solar energy collected by solar stills for desalination by membrane distillation, Renew. Ener. 25 (2002) 293–305.
[27] L. Kirkup, R.B. Frenkel, An introduction to uncertainty in measurement, Cambridge University Press, Cambridge, 2006.

Appendix A

The trans-membrane flux J was calculated by

$$J = \frac{m_w}{A_m \tau} = \frac{\frac{\pi}{4} D_i^2 \cdot \frac{p_{d2} - p_{d1}}{\rho_w g} \cdot \rho_w}{A_m \tau} = \frac{\pi D_i^2 (p_{d2} - p_{d1})}{4 g A_m \tau} \ [\mathrm{kg/m^2\ h}] \tag{A1}$$

where m_w is the mass of produced water, A_m is the membrane area, τ is the operation time, D_i is the inner diameter of the distillate tank, p_{d1} and p_{d2} are the readings of the differential pressure transmitter at the beginning and the end of the experimental period, ρ_w is the density of produced water, and g is the acceleration of gravity. The recovery ratio λ was calculated by

$$\lambda = \frac{m_w}{V_f \rho_f \tau} = \frac{\frac{\pi}{4} D_i^2 \cdot \frac{p_{d2} - p_{d1}}{\rho_w g} \cdot \rho_w}{\frac{\pi}{4} d_i^2 v_f \rho_f \tau} = \frac{D_i^2 (p_{d2} - p_{d1})}{d_i^2 v_f \rho_f \tau g} \tag{A2}$$

where V_f is the volume flow of feed, ρ_f is the feed density, d_i is the inner diameter of feed pipe, and v_f is the flow velocity read from the flow meter.

According to the uncertainty propagation formula introduced by Kirkup and Frenkel [27], if a parameter y is the function of a series of measured independent variables, $x_1, x_2, \ldots, x_\mathrm{n}$,

$$y = f(x_1, x_{2,} \ldots, x_n) \tag{A3}$$

the uncertainty of y, expressed as u(y), can be calculated from the uncertainties of the measured variables, $u(x_1)$, $u(x_2)$,..., $u(x_\mathrm{n})$,

$$u(y) = \sqrt{\left(\frac{\partial y}{\partial x_1}\right)^2 u^2(x_1) + \left(\frac{\partial y}{\partial x_2}\right)^2 u^2(x_2) + \cdots + \left(\frac{\partial y}{\partial x_n}\right)^2 u^2(x_n)} \tag{A4}$$

Based on Eqs. (A1)–(A4), the uncertainties of the trans-membrane flux J and the recovery ratio λ of VMD were estimated to be $\pm 0.014\ \mathrm{kg/(m^2\ h)}$ and ± 0.0005, respectively. Within the parameter range of $T_\mathrm{hf} = 55$–$75\,^\circ\mathrm{C}$, $p_\mathrm{v} = 0.01$–$0.02\ \mathrm{MPa}$, $F_\mathrm{f} = 70$–$110\ \mathrm{L/h}$, and $C_\mathrm{f} = 30$–$45\ \mathrm{g/kg}$, the relative uncertainty of both the indexes was lower than 5%.